

# CONTROL OF CONVECTIVE FLOWS IN A RECTANGULAR CRUCIBLE BY A SPECIAL TYPE OF ELECTROMAGNETICAL STIRRING

NEGRILA R.A., POPESCU A., PAULESCU M., VIZMAN D.

Faculty of Physics, West University of Timisoara, Bd. V. Parvan 4, 300223 Timisoara, Romania

e-mail address of corresponding author: [negrila.andrei.radu@gmail.com](mailto:negrila.andrei.radu@gmail.com)

**Abstract** : One of the key issues in the technology development of directional solidification (DS) of silicon for photovoltaic applications is to control the interface shape and impurities distribution through tailoring the melt convection. In this view a new type of melt flow control through electromagnetic stirring (EMS) for the DS of silicon is proposed. To show the potential of the EMS method both numerical and experimental investigations were performed in a model experiment for a GaInSn melt. The computed velocities were studied and compared to experimental Doppler ultrasound velocity profiles.

## 1. Introduction

In directional solidification (DS), which is the main method for growing photovoltaic silicon, accounting for over 50% of the world market share, a major role in heat and species transport is played by the melt convection. Some previous contributions [1-7] show that melt convection plays a crucial role for the heat transfer, solid-liquid interface shape (and thus for thermal stress and dislocations) and for the distribution of impurities and dopants. In DS the buoyant (or natural) convection, has positive effects on the crystalline quality of the ingot by reducing the segregated impurity diffusion boundary layer in front of the growth interface and thus homogenizing the impurity distribution inside the melt. Therefore, the impurity concentration incorporated into the crystal is reduced and unwanted effects such as morphological destabilization of the crystalline growth interface or impurity precipitate formation in the melt are usually avoided.

However, there are some limitations to the effectiveness of buoyant convection. Precipitates tend to be formed and incorporated into the growing silicon lattice between buoyant convection loops [8,9]. Another limitation is the formation of a poorly mixed area in the center of the melt, separating natural convection structures from the melt surface and crystal interface [7], which favors precipitate formation there. Also, with the increase of crucible dimensions, the control of melt flow in a beneficial way becomes a very challenging task. In recent years, some techniques have been proposed in order to tailor melt flow in a DS process. Some of them are based on travelling [10-12] or rotating [13-15] magnetic fields; others on a mix between vertical magnetic field and electrical current [16, 17] and another on mechanical stirring [18].

Based on the idea of melt stirring from Electromagnetic Czochralski method developed by Watanabe et al [19], numerical modeling was carried out in the case of DS, for a similar configuration with one electrode placed in a vertical magnetic field [16]. Due to practical crystal growth reasons, a new configuration for melt flow control (EMS), with two electrodes in contact with the melt placed in a vertical magnetic field, was investigated by numerical simulation in [17] and found to be very effective.

## 2. Numerical model and experimental set-up

In order to validate the numerical modeling for this method of electromagnetic stirring, both numerical and experimental investigations have been carried out on a model experiment in an isothermal square-shaped crucible, where a room temperature liquid alloy mimics a silicon melt inside a DS set-up. Two types of electrodes configurations were considered:

- a symmetric configuration (SC) with the two electrodes placed along a diagonal, symmetric from the central point, at a third diagonal length from the corner point (fig 1b)
- an asymmetric configuration (AC) with one electrode placed in the center of the free melt surface and the second one placed on a diagonal closer to the corner point at the third distance between the center and the corner point (fig 1c)

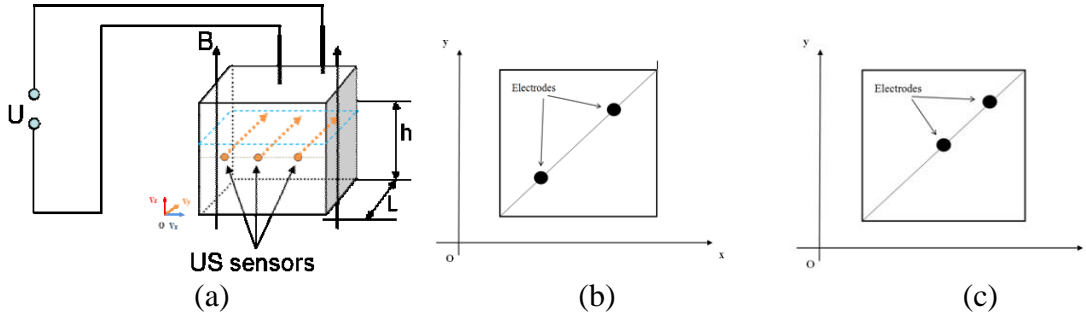


Figure 1: (a) Crucible geometry for 3D modeling of GaInSn melt stirring, using a vertical magnetic field combined with an electrical DC current, induced into the melt by: (b) 2 symmetrical electrodes, (c) 2 asymmetrical electrodes.

The melt flow is described by the three-dimensional time-dependent equations of mass and momentum conservation:

$$\nabla \cdot \mathbf{u} = 0 \quad (1)$$

$$\rho \frac{\partial \mathbf{u}}{\partial t} + \rho (\mathbf{u} \cdot \nabla) \mathbf{u} - \mu \nabla^2 \mathbf{u} = -\nabla p + \mathbf{f}_L, \quad (2)$$

where  $\rho$  is the density,  $\mathbf{u}$  the melt velocity,  $p$  is the pressure,  $\mathbf{j}$  is the electric current density,  $\mathbf{B}$  is the magnetic field induction. The influence of the steady magnetic field on the melt flow is considered by the Lorentz force density  $\mathbf{f}_L = \mathbf{j} \times \mathbf{B}$  in the Navier-Stokes equations. For the calculation of the Lorentz force, the electric current density  $\mathbf{j} = \sigma (-\nabla \Phi + \mathbf{v} \times \mathbf{B})$  induced in the melt is taken into account, where  $\sigma$  is the electric conductivity,  $\mathbf{v}$  is the melt velocity and  $\Phi$  the scalar electrical potential.  $\Phi$  is calculated by an additional differential equation obtained from the electrical current continuity equation:

$$\nabla \cdot \mathbf{j} = 0 \rightarrow \Delta \Phi = \nabla \cdot (\mathbf{v} \times \mathbf{B}) \quad (3)$$

The crucible walls and melt free surface are considered to be electrical isolated. Therefore  $\nabla \Phi \cdot \mathbf{n} = 0$  on all boundaries except the surface elements, where the electrodes touch the melt, where  $\nabla \Phi \cdot \mathbf{n} = -j_n / \sigma$ , with  $j_n$  the density of the electrical current. The magnetic field imposed is vertical and constant, independent of the melt rotation. The auto-induced magnetic field generated by the electrical current is not taken into account in the numerical model, as its influence is very small for the modeled values of  $I$  and  $B$ . The melt flow velocities along the boundaries at the crucible and at the crystal are set to  $\mathbf{v} = \mathbf{0}$  (no-slip). Along the free surface of the melt, „no shear stress” condition is considered. The simulation has been performed using the STHAMAS3D software. The computational domain is 70 x 70

x 50 mm<sup>3</sup> in size consisting of a block with a non-orthogonal grid that has a local refinement at the walls in order to resolve the boundary layers. The mesh in the melt consists typically of 180000 control volumes, which is assumed to be sufficient to resolve the main features of the flow. In order to obtain a realistic solution starting from an arbitrary initial solution at least 900 sec real time were computed with a time step of 0.1 sec.

In order to validate the numerical simulation, an experimental model was developed (fig 2), consisting of a square-shaped plexiglas crucible (70 x 70 x 70 mm<sup>3</sup>) placed in a vertical magnetic field. The crucible contains a 50 mm high GaInSn room temperature liquid alloy, which has similar material properties to molten Silicon. Two electrodes are in contact with the alloy melt surface, through which a direct current passes. Velocity profiles are measured by Ultrasound Doppler Velocimetry (UDV) with ultrasonic transducers being placed perpendicular on the plexiglas crucible surface at 3 different positions for one flow plane at a time (fig 1 a, fig 2). The experimental velocity profiles are then compared to numerical ones extracted from the simulations, which correspond to the same position.

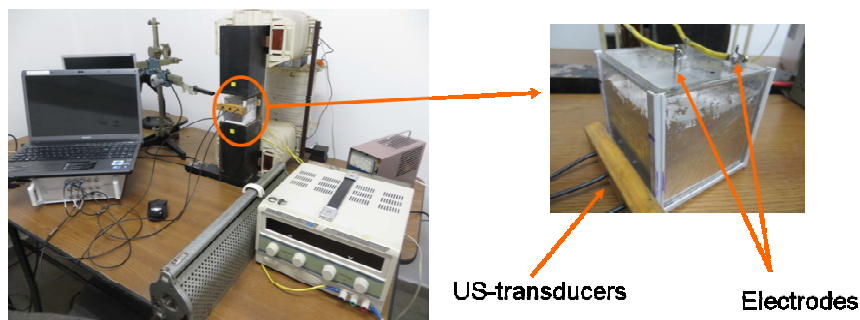


Figure 2: EMS model experiment set-up with a GaInSn melt in a plexiglas crucible connected through electrodes to a DC source and placed inside an electromagnet's vertical magnetic field.

### 3. Results and discussions

The combination of a vertical magnetic field and radial components of the electrical current generates a Lorentz force distribution inside the melt, which gives rise to different flow structures, depending on electrical current intensity, magnetic field induction and electrode positioning.

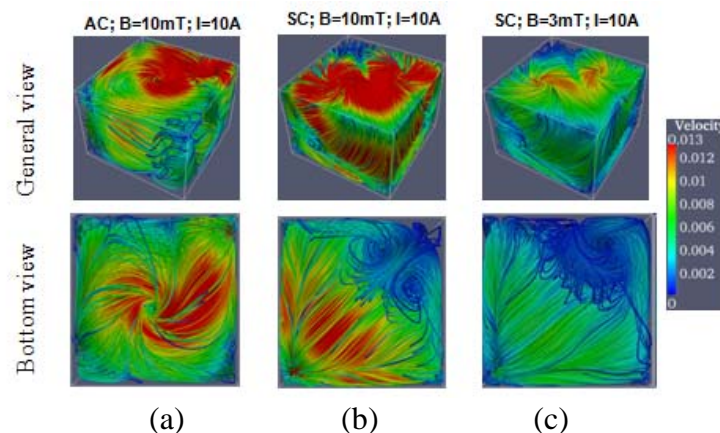


Figure 4: Flow structures particle tracking for: (a) asymmetrical electrodes position at I = 10 A, B = 10 mT; (b) symmetrical electrodes position for I = 10 A, B = 10 mT; (c) symmetrical electrodes position for I = 10 A, B = 3 mT.

The flow structure depends on the electrodes positioning. It can be seen from fig 4a that, in the case of an asymmetrical electrode positioning, the flow structure is dominated by an azimuthal rotation around the central electrode, while in the case of the electrodes symmetrical positioning (fig 4b,c), the flow structure changes from a spiraling rotation around the two electrodes at the top to a meridional recirculation at the bottom. It is also a notable fact that the melt stirring is also strong for a magnetic field of just 3 mT (fig 4c).

Using the experimental set-up described in section 2, velocity profiles have been obtained through the ultrasound Doppler velocity profile method, in order to validate the numerical model. The main area of interest presented here is the region close to the bottom of the crucible, which is chosen because it is important to see if the flow is strong enough at the melt-crystal growth interface to avoid impurity accumulation in the boundary layer in front of it.

In fig 5, the velocity field from the 45 mm height plane is represented. At this plane velocity profiles taken from 7 mm, 35 mm and 63 mm from the edge are compared with the ones measured in the experiment at the same position. The experimental values represent the flow velocity projection on the US beam axis. By convention, a negative velocity is oriented towards the US transducer, while a positive one points away from it. The experimental results show a better agreement for the AC case (fig 5a), where the flow structure is simpler than for the SC one (fig 5b). The velocity in a point from the experimental profiles represents the average velocity in a volume centered in that point, which is limited by the lateral US beam divergence. Therefore, if the spatial velocity gradient is higher (associated to a more complex flow structure like in the SC case) the average velocity volume is farther away from the point value taken from the simulation. Also, the material constants may vary slightly in reality from the values considered in the simulations and this, along with the auto-induced magnetic field, can also be a cause of the differences between numerical model and experiment.

As was observed from the flow structures particle tracking in fig 4, the experimental results also show that for the AC the rotation set in motion at the electrodes level goes down all the way to the bottom, while it changes from top to bottom for the electrodes SC.

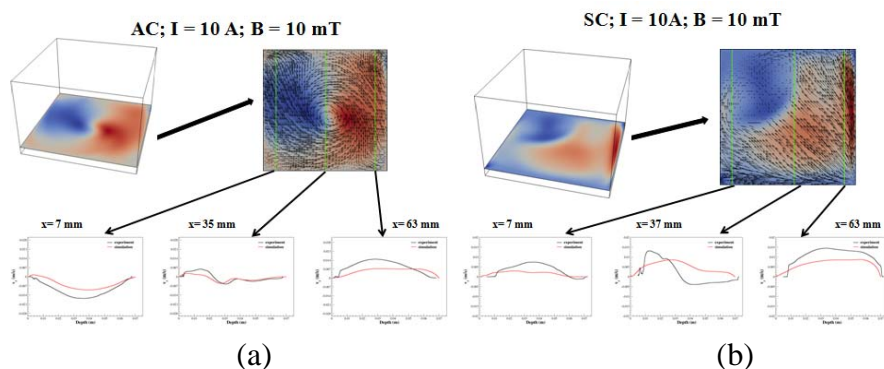


Figure 5: Experimental and numerical velocity profiles at 10 A, 10 mT compared for :  
(a) asymmetrical case; (b) symmetrical case.

#### 4. Conclusions

It was found that even a small magnetic field (3-10 mT) and an electrical current in the electrodes of maximum 10 A can produce a significant stirring effect. Melt rotation develops in the whole mass of the melt, which could have a beneficial effect for the application of this technique to silicon DS for photovoltaic applications. This is important because it could be more cost effective to implement a smaller magnetic field inside a DS furnace, or maybe use

the magnetic field generated by the induction coils in the cases where the furnace uses inductive heating. The numerical results for the melt convection (intensity and flow patterns) are in good agreement with the experimental findings. The results prove the potential of the proposed method to control convective flows in a rectangular crucible relevant for the silicon DS method.

## 5. References

- [1] Reimann, C.; Trempa, M.; Jung, T.; Friedrich, J.; Müller, G.: Modeling of incorporation of O, N, C and formation of related precipitates during directional solidification of silicon under consideration of variable processing parameters. *Journal of Crystal Growth* 312 (2010) 878–885.
- [2] Chen, X.; Nakano, S.; Kakimoto, K.: Three-dimensional global analysis of thermal stress and dislocations in a silicon ingot during a unidirectional solidification process with a square crucible. *Journal of Crystal Growth* 312 (2010) 3261–3266.
- [3] Vizman, D.; Friedrich, J.; Müller, G.: 3D time-dependent numerical study of the influence of the melt flow on the interface shape in a silicon ingot casting process. *Journal of Crystal Growth* 303 (2007) 231–235.
- [4] Miyazawa, H.; Liu, L.; Hisamatsu, S.; Kakimoto, S.: Numerical analysis of the influence of tilt of crucibles on interface shape and fields of temperature and velocity in the unidirectional solidification process. *Journal of Crystal Growth* 310 (2008) 1034–1039.
- [5] Kuliev, A.T.; Durnev, N.V.; Kalaev, V.V.: Analysis of 3D unsteady melt flow and crystallization front geometry during a casting process for silicon solar cells. *Journal of Crystal Growth* 303 (2007) 236–240.
- [6] Teng, Y.; Chen, J.; Lu, C.; Chen C.: The carbon distribution in multicrystalline silicon ingots grown using the directional solidification process. *Journal of Crystal Growth* 312 (2010) 1282–1290.
- [7] Popescu, A.; Vizman, D.: Numerical Study of Melt Convection and Interface Shape in a Pilot Furnace for Unidirectional Solidification of Multicrystalline Silicon. *Crystal Growth and Design* 12 (2012) 320–325.
- [8] Pihan, E. et al.: Influence of Lateral Temperature on Light Elements Precipitations during MC-SI Crystallization in a DS Furnace. 26th EU PVSEC Conference (2011), 1900 - 1903
- [9] Zheng, L.; Ma, X.; Hu, D.; Zhang, H.; Zhang, T.; Wan, Y.: Mechanism and modeling of silicon carbide formation and engulfment in industrial silicon directional solidification growth. *Journal of Crystal Growth* 318(2011), 313–317.
- [10] Rudolph, P.: Travelling magnetic fields applied to bulk crystal growth from the melt: The step from basic research to industrial scale. *Journal of Crystal Growth* 310 (2008) 1298–1306.
- [11] Dropka, N.; Frank-Rotsch, Ch.; Miller, W.; Rudolph P.: Influence of travelling magnetic fields on S–L interface shapes of materials with different electrical conductivities. *Journal of Crystal Growth* 338 (2012) 208–213.
- [12] Dadzis, K.; Ehrig, J.; Niemietz, K.; Patzold, O.; Wunderwald, U.; Friedrich, J.: Model experiments and numerical simulations for directional solidification of multicrystalline silicon in a traveling magnetic field. *Journal of Crystal Growth* 333 (2011) 7–15.
- [13] Griffiths, W.D.; McCartney, D.G.: The effect of electromagnetic stirring during solidification on the structure of Al-Si alloys. *Materials Science and Engineering A* 216 (1996) 47–60.
- [14] Willers, B.; Eckert, S.; Michel, U.; Haase, I.; Zouhar, G.: The columnar-to-equiaxed transition in Pb–Sn alloys affected by electromagnetically driven convection. *Materials Science and Engineering A* 402 (2005) 55–65.
- [15] Willers, B.; Eckert, S.; Nikrityuk, P.A.; Rübiger, D.; Dong, J.; Eckert, K.; Gerbeth, G.: Efficient Melt Stirring Using Pulse Sequences of a Rotating Magnetic Field: Part II. Application to Solidification of Al-Si Alloys. *Metallurgical and Materials Transactions B* 39 (2008) 304–316.
- [16] Tanasie C.; Vizman D.; Friedrich J.: Numerical study of the influence of different types of magnetic fields on the interface shape in directional solidification of multi-crystalline silicon ingots. *Journal of Crystal Growth* 318 (2011) 293–297.
- [17] Vizman D.; Tanasie C.: Novel method for melt flow control in unidirectional solidification of multi-crystalline silicon. *Journal of Crystal Growth* 372 (2013) 1–8.
- [18] Dumitrica, S.; Vizman, D.; Garandet, J.-P.; Popescu, A.: Numerical studies on a type of mechanical stirring in directional solidification method of multicrystalline silicon for photovoltaic applications. *Journal of Crystal Growth* 360 (2012) 76–80.
- [19] Watanabe M.; Eguchi M.; Hibiya T.: Silicon Crystal Growth by the Electromagnetic Czochralski (EMCZ) Method. *Japanese Journal of Applied Physics* 38 (1999) 10-13